J. Cosmet. Sci., 66, 31–56 (January/February 2015)

Prediction of bending set, wave efficacy, and hair damage using an extensional permanent waving treatment and the 20% index value

YUZO UENO and HIDEO NAMIKI, *Department of Biology, School of Education, Waseda University, Tokyo, Japan*.

Accepted for publication November 23, 2014.

Synopsis

To predict "wave efficacy" as evaluated by hairdressers, an extensional permanent waving treatment was performed on human hair fibers using various wave lotions manufactured in Japan. Glass columns devised for the purpose were equipped with a tensile tester in order to increase the measurement accuracy. Notably, the observed set agreed with the theoretical set. In addition, the data for the extensional set exhibited good correlation with the bending set and the wave efficacy assessed in a beauty parlor, and hair damage was estimated by the characteristic change in the 20% index. The following facts were experimentally determined. First, the Young's modulus of the hair fibers after extensional permanent waving treatment continually decreased with an increase in the reduction of the fibers and then abruptly decreased at 80% reduction. Second, the reduction of hair treated with the ammonium salt of thioglycolic acid followed pseudo first-order kinetics only during the initial stage of the reaction, independent of the pH level. Third, the 20% index of the individual virgin hairs remained constant in water at 30°C and also correlated with the Young's modulus of the hair after extensional permanent waving treatment.

INTRODUCTION

Many studies regarding the physical and chemical treatment of wool and human hair have been presented and reviewed by Arai (1) and Robbins (2). However, these studies provide limited information that hairdressers can apply to practical permanent waving treatments in actual beauty parlors. There is a significant need in beauty parlors to be able to predict wave efficacy using a given wave lotion and estimate hair damage.

The purpose of the present study was to achieve this goal using a simple method. Therefore, quick extensional permanent tests were performed using commercially available wave lotions under conditions that simulated treatments given in beauty parlors, and the results were used to predict the bending set and wave efficacy and determine the 20% index (3) for hair damage.

Address all correspondence to Yuzo Ueno at yuzo@hm.catv.ne.jp.

The position of the extensional permanent test was similar to that used by Wortmann (4), who combined a static extensional permanent test with a dynamic method (5,6) and performed a bending test using hairs as loops hair. However, Wortmann reported only a modest correlation between the bending and extensional properties, suggesting that the desired goal of the present study does not seem to be possible.

Therefore, the extensional permanent tests were performed using only the static method and a specially devised apparatus equipped with a tensile tester. In addition, the bending tests were performed in a carefully designed vessel in order to increase accuracy. The results obtained using this approach were then compared to Wortmann's results.

Hair damage due to permanent treatment was defined as the ratio of the values for the Young's modulus after and before treatment, and the 20% index values were used to estimate the hair damage.

EXPERIMENTAL METHODS

All experiments were conducted on chemically untreated Japanese hair (except for the hair used in the hair-damage tests) obtained from "BOY beauty parlor" located in Japan. The hair fibers were cleaned with a 1 g/100 g aqueous solution of sodium lauryl sulfate for 30 min, rinsed with de-ashed water for 1 h at room temperature, and then allowed to dry under ambient conditions. Single straight-hair fibers with diameters of 55–70 μm were selected for the tests. Table I provides the origins and characteristics of the commercial wave lotions used in the tests. Manufacturers A, B, and C were selected as representative manufacturers in Japan, and each manufacturer typically provides three product grades listed as S, N, and W, representing different molding strengths: strong, neutral, and weak, respectively. An aqueous solution (8 g/100g $NaBrO_3$, pH 7.0) was applied as a neutralizer in all of the experiments. Deashed water was used in all the experiments.

Table I
Commercial Wave Lotions Used in Experiment

	Manufacturer		Composition of sample			
Sample	(Waving lotion)	Grade	pH	TGA (g/100g)	DTDG (g/100g)	Buffer system
A-S	Manuf. A	S	9.1	6.8		
A-N	Manuf. A	N	8.6	6.5		NH_3/NH_4HCO_3
A-W	Manuf. A	W	8.5	5.0		
B-S	Manuf. B	S	8.8	6.2		
B-N	Manuf. B	N	8.6	9.6	3.6	MEA/NH_4HCO_3
B-W	Manuf. B	W	8.0	6.4		
C-S	Manuf. C	S	8.6	7.0		
C-N	Manuf. C	N	7.8	6.8		NH_3/NH_4HCO_3
C-W	Manuf. C	W	8.0	5.6		

S, N, and W, strong, neutral, and weak strength of the wave lotions for molding; TGA, ammonium salt of thioglycolic acid; DTDG, ammonium salt of dithiodiglycolic acid; MEA, monoethanolamine (2-aminoethanol). Analyzed according to the Japanese Standard for Permanent Waving Agents MHW amended Notification No. 166, October 14, 1985.

EXTENSIONAL SETTING TEST

The extensional setting experiments were performed on single hair fibers in specially devised columns equipped with tensile tester (TENSILON UT-1-4-1, Toyo Baldwin, Tokyo, Japan).

The columns are shown in Figure 1, and the experimental procedure is described schematically in Figure 2.

The procedure of the extensional setting test was basically the same as that used by Wortmann. However, there were some differences between the two methods.

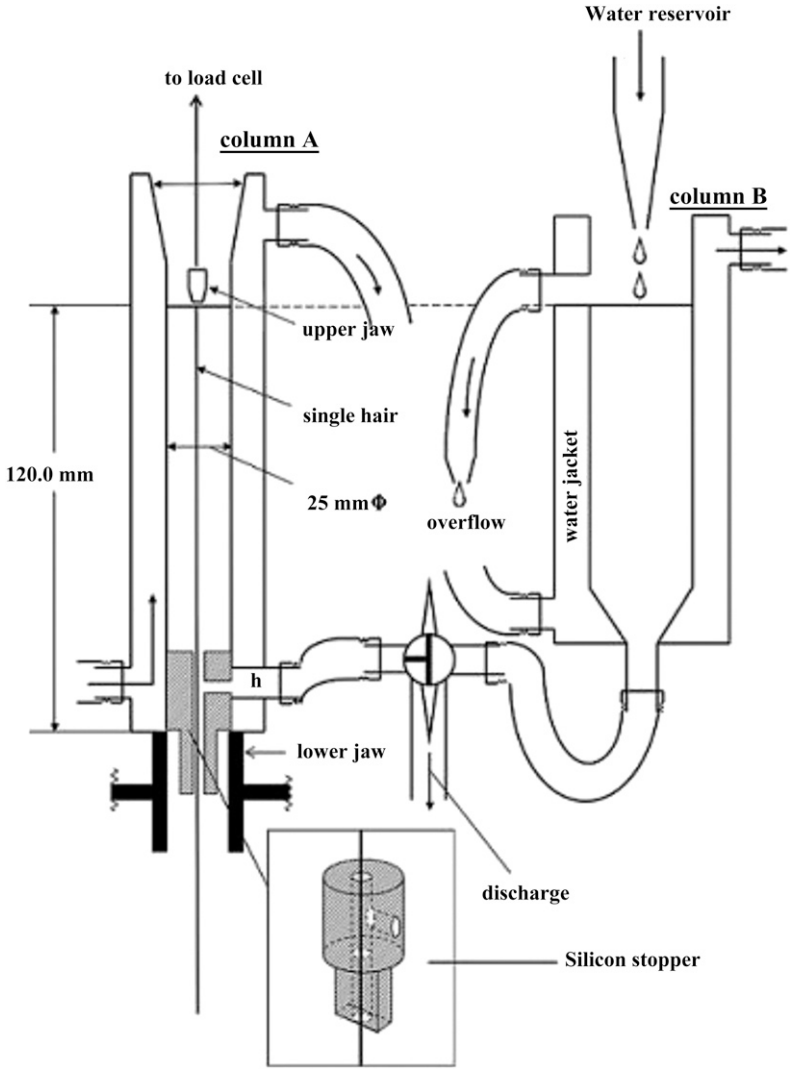

Figure 1. Apparatus used for the extensional permanent treatment. Column A is positioned on the lower jaw of the cross head of the tensile tester. Column B ensures a constant water level in Column A, such that the 20% index can be measured. Then, both columns A and B are combined and filled with water.

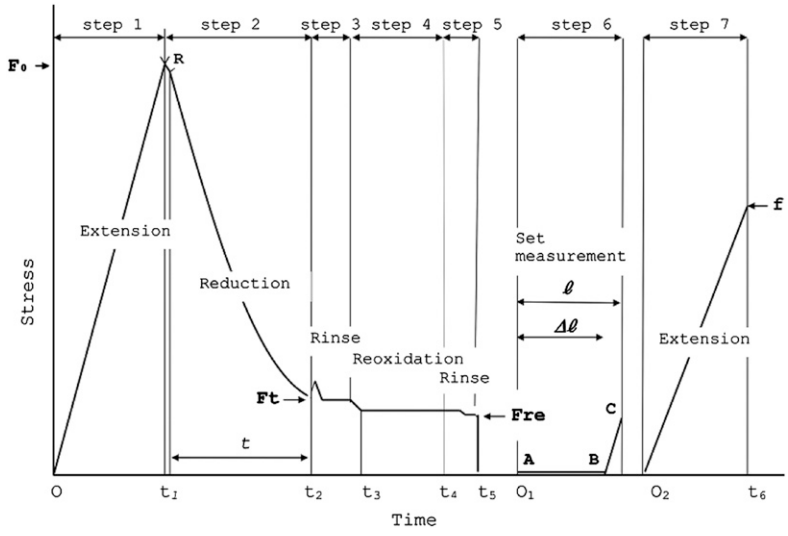

Figure 2. Graphical depiction of the procedure adopted for measuring the extensional permanent treatment. Typical experimental curve obtained for a static extensional permanent treatment.

First, the pretreatment of the hair was different. Wortmann conducted a stress–strain test in water with the hair held in the shape of the desired curve. The hair was then restored to its normal condition and mounted as a loop. Subsequently, the hair was relaxed for 20 min and then extended by 0.5%, after which the reduction/rinse/reoxidation/rinse sequence was initiated. In the present study, after selecting straight hairs and measuring their diameters, the fibers were extended by 1.5% in water and then the reduction/rinse/reoxidation/rinse sequence was immediately initiated. In addition, the hairs were not mounted as loops; rather, each single hair was exactly fixed to 120.0 mm as the original length to be extended before being placed in water. Thus, the hairs were not relaxed in water for 20 min followed by reduction with physical relaxation of the hair. The differences in the procedures are due to the fact that in the present study, the aim was to simulate the actual process used in beauty parlors.

Second, the method used to determine the set length during the extensional test was different. Wortmann determined the initial extended length and the set length after treatment by extrapolating the stress–strain curve to zero. We determined these lengths by direct measurement of the extended and set lengths using a method developed in house (see Step 6: Measurement of the set length).

Third, the method for measuring the Young's modulus of the hairs after treatment was different. Wortmann determined the value of the Young's modulus using a dynamic method. In the present study, a static method performed under the same conditions as those used to measure the stress in water was employed (see section Step 7: Extension).

Prior to the experiments, experimental column and single wet hair fiber were prepared as described in the following section.

Experimental column equipment. Specially designed experimental equipment was used for this study. As can be seen in Figure 1, glass columns A and B were connected via a tube

attached to the bottom of each column. Column A was mounted on the lower jaw of the cross head of a tensile tester, and Column B was mounted on a stand with which the height of the column could be controlled.

A single straight hair was exactly fixed down the middle of Column A through a silicon stopper. Column A could be separated from Column B by shutting the lower jaw and closing the three-way stopcock. All permanent treatments of the fibers were conducted in Column A.

Column B was used to adjust the water level of Column A during measurement of the 20% index. Because the water level in Column A rose and fell with the movement of the cross head, the water level in Column A was kept constant by using Column B as an overflow system for measuring the 20% index. The temperature of the solution in the columns was maintained at 30°C using water circulating at a constant temperature through a jacket surrounding the columns.

Fixing a single wet hair fiber in the experimental apparatus. First, the standard position for the test was determined by placing a 120.0-mm-high metal block on the lower jaw and adjusting the position of the cross head such that the distance between the edge of the upper and lower jaws could be set exactly at 120.0 mm, as shown in Figure 1. Second, one end of the hair fiber was connected to a 100-g load cell using the upper jaw, and the other end was passed through the fine path of the silicon stopper and connected to a small 0.5-g weight in order to straighten the fiber. After shutting the lower jaw using 3.0 kg/cm^2 of air pressure and closing the three-way stopcock, Column A was filled with water. The straight hair fiber was loosened in the water for 5 min. The water was then discharged, the lower jaw opened, and the wet fiber was allowed to straighten. Subsequently, the lower jaw was shut and, if the fiber loosened, the lower jaw was opened and the cross head was moved to a slightly higher position, whereupon the lower jaw was again shut at this position and the cross head was moved down such that the wet fiber could be fixed at the standard position without slack.

By repeating this procedure through trial and error, the standard conditions for a 120.0-mm–long fiber tensioned without slack in water with zero strain and stress at the standard position was satisfied.

Treatment procedure as illustrated in Figure 2.

Step 1: Extension. The tensile tester was programmed to extend a single hair fiber by 1.8 mm (1.5% of the original length) at a rate of 5.0 mm/min in water (1.5% extension) and return to its original position.

The extension was recorded at 200 mm/min on recording paper to confirm the accuracy of the extended length. The value "Fo" measured here was regarded as an index of the Young's modulus of the fiber before permanent treatment.

Step 2: Reduction. While retaining the strain, the water was discharged by opening the stopcock, and after the stopcock was closed again, a given waving lotion was immediately poured into the mouth of the column. Relaxation began at the point labeled "R" in Figure 2, and the stress gradually decayed (recording speed: 10 mm/min). At a reduction time t (min), the waving lotion was discharged. The value Ft measured here was the apparent residual stress due to reduction and included the swelling stress.

Step 3: Rinse. After the waving lotion was discharged, the column was repeatedly filled with water and discharged five times, following which the fiber was immersed in water for 10 min (recording speed: 2 mm/min).

Step 4: Reoxidation. The neutralizer was poured into the column, and the fiber was immersed for 15 min (recording speed: 2 mm/min).

Step 5: Rinse. The neutralizer was discharged and the reoxidized fiber was rinsed and immersed in water for 5 min (recording speed: 2 mm/min).

Step 6: Measurement of the set length. The strain reduced to zero (i.e., the original position), and the treated fiber was loosened in water. After marking the starting point (A) on the recording paper, recording speed was set to that used in Step 1 (200 mm/min) and the fiber was extended again by 1.5% under the same conditions as those described in Step 1. The set length (loosened length) was extended in the absence of stress until point B was reached (i.e., in the range from A to B over an extension length $\triangle\ell$). The stress appeared at point B and increased until point C was reached, which corresponded to a 1.5% extension relative to the original length [i.e., in the range from A to C, over an extension of length (ℓ)]. The values for $\triangle\ell$ and ℓ measured in this way provided the observed set values Sℓ(ext) (%) for the extensional setting experiment as follows:

$$S\ell\ (\text{ext}) = \triangle\ell/\ell \times 100\ (\%), \tag{1}$$

where $\triangle\ell$ is the observed set length and l is the observed extended length.

Step 7: Extension. The water was discharged, the lower jaw opened, and the cross head returned to the original position. The treated fiber was then fixed at the standard length in water under the same conditions as those used in Step 1 (recording speed: 200 mm/min), and "f" was measured as an index of the Young's modulus after treatment.

Graph of the reduction progress versus time (Pa/t curve). The data required for establishing the Pa/t curves were obtained independently of the above results using only Steps 1 and 2 and omitting all subsequent procedures (Steps 3–7). These measurements were repeated six times using six different single fibers. The relaxation curve obtained in Step 2 was converted to the apparent progress of reduction, Pa (%), of the hair fiber with respect to time as follows:

$$\text{Pa} = \{1 - (\text{Ft}/\text{Fo})\} \times 100\ (\%), \tag{2}$$

where Ft is the residual stress at *t* min during reduction (see Step 2) and Fo is the index of Young's modulus before reduction. Note that the measured stress includes swelling due to the waving lotion, and thus the value for Pa calculated using equation (2) is referred to as the apparent progress of reduction.

Ft was measured from the height of the relaxation curve once every minute using a slide caliper. The values for Fo and Ft at each time obtained for the six different hair fibers were, respectively, averaged, and the mean values were then substituted into equation 2. The calculated average Pa values were then plotted versus time to generate "Pa/t curves," which were used to characterize the different waving lotions.

BENDING SET EXPERIMENT

Wortmann determined the bending set by winding hairs as loops on a cylindrical roller and cutting the loops and measuring the fiber set by observing how much loop initial

form is remained. In our method, a single hair was used and the bending set was measured using the devised apparatus as follows.

In the bending set experiment, a single hair fiber was placed on the bending apparatus in the manner illustrated in Figure 3. The fiber was equipped with small weights at both ends and was wound at the root of a 10-mm-diameter cylinder on the device shown in the figure and vertically held in water at 30°C for 5 min. While holding the fiber in water, the four nuts were evenly tightened to fix the fiber onto the device. The weights were then removed and the water on the surface of the device was wiped off. The device fixing the wet fiber was then placed into a 100-ml beaker containing 50 ml of a given waving lotion for t min, and subsequently the device was treated in the prepared beaker under the same conditions as those described in Steps 3, 4, and 5 as shown in Figure 2.

When the treatment was finished, the fiber was cut at the point of intersection, separated from the device, and immediately transferred into a Petri dish filled with water at 30°C. The Petri dish was then placed on a photocopy machine. By covering the fiber within the Petri dish with a white PVC disk, a good quality photocopy could be obtained. The photocopy of each bending treated fiber was in the shape of an arc, and the radius of the arc

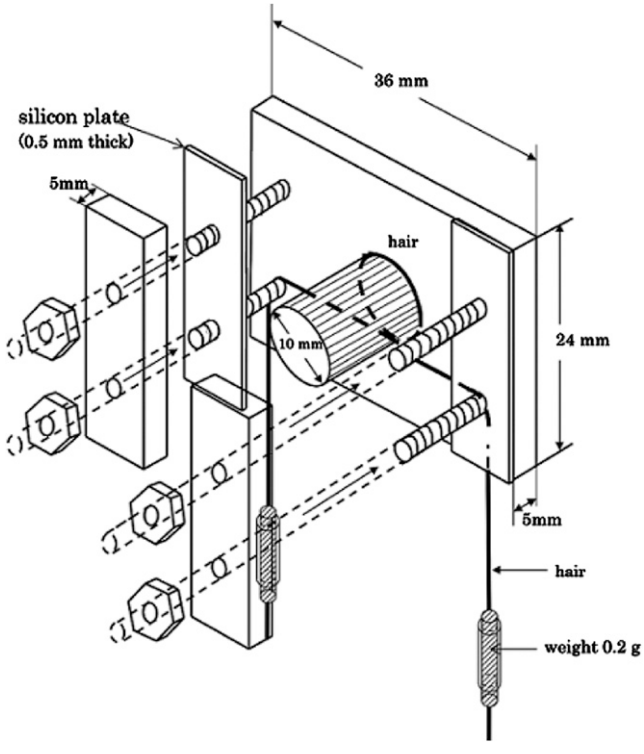

Figure 3. Device used for the permanent treatment of the bending set. A single wet hair wound at the root of the cylinder and fixed using silicon plates that are tightened to the screws by four bolts.

was measured from a copy enlarged by 100%. The extent of the bend induced by the bending treatment, Sℓ (bend) (%), was calculated as follows:

$$S\ell(\text{bend}) = (5.0/r/2) \times 100\%, \quad (3)$$

where r is the bend radius of the fiber derived from the doubly enlarged copy.

WAVE EFFICACY IN A BEAUTY PARLOR

Practical treatment measurements were performed by a proficient hairdresser, and the results were reported to us. A small tissue wound on a rod was treated, and the resulting assessment, referred to as the "wave efficacy," was calculated using the spiral tissue length, length of the wave and diameter of the rod:

$$\text{wave efficacy} = 100 \times N \times D/\ell, \quad (4)$$

where l is the length of the spiral tissue, N is the wave length, and D is the diameter of the rod.

MEASUREMENT OF THE 20% INDEX

The path connecting the water contained in columns A and B was opened by operating the three-way stopcock, and both columns were filled with water in order to maintain a constant water level in Column A. The tensile tester was programmed to alternately load a 20% strain and then unload to the original position at a rate of 5 mm/min. The resulting hysteresis curve provided the 20% index.

MICROSCOPY OF CROSS SECTIONS OF THIOGLYCOLATE-TREATED HAIRS

White hair fibers were cleaned with a 1 g/100 g lauryl sulfate aqueous solution, washed with water, immersed for 3 min, wiped with paper, followed by immersion in the respective reducing agent (0.6 M, pH 8.6) for 5 min. The reduced fibers were washed with deashed water for 3 min and subsequently dried at room temperature.

Thioglycolate-treated hairs were cryoprotected in a graded series of sucrose (5, 10, and 20% in a 0.1 M phosphate buffer, pH 7.3) on ice and embedded in optimal cutting temperature compound (Sakura Finetechnical Co. Ltd., Tokyo, Japan) before freezing on a metal block prechilled with liquid nitrogen. Frozen hairs were cross sectioned in 10-μm thick sections in a Cryostat (Leika CM 1850, Nussloch, Germany), air-dried on microscopic slides, and post-fixed in 4% paraformaldehyde dissolved in a 0.1 M phosphate buffer (pH 7.3) for 5 min. The sections were prewashed in a 0.1 M TrisHCl buffer at pH 9.5, stained with 0.1% methylene blue for 5 min, and then rinsed in the same buffer. Microscopic images were captured under epi illumination using a Nikon E600 optical system (Nikon Instech Co. Ltd., Tokyo, Japan) equipped with an Olympus DP70 camera (Olympus, Tokyo, Japan). The captured images were density scanned on a computer using a National Institute of Health (NIH) Image analyzer with the aid of a software by Celisene Olymoas Co. Ltd (Tokyo, Japan).

DETERMINATION OF THE DISTRIBUTION OF HG (IN FORMED S–HG–S BONDS) IN HAIR

To determine the distribution of Hg (in formed S–Hg–S bonds) in the hair fibers, each treated hair fiber was embedded in an epoxy resin (EPON812; Taab Co. Ltd., West Berkshire, UK) and cut into 0.1-μm thick cross sections using an ultramicrotome (Leica EM UC7; Leica Microsystems Ltd., Vienna, Austria). The Hg count (Lα) was measured at 44 points along the diameter of the cross-sectioned fiber via energy dispersive x-ray (EDX) spectroscopy using a field emission transmission electron microscope (FE-TEM; Hitachi HF-2200, Tokyo, Japan) (7)

PREPARATION OF SODIUM AND AMMONIUM THIOGLYCOLATE SOLUTION (0.6 M, PH 8.6)

Thioglycolic acid (analytical grade reagent; Wako Co. Ltd., Tokyo, Japan) was dissolved with water, and pH was adjusted with $NaOH/NaHCO_3$ for sodium thioglycolate and with NH_3/NH_4CO_3 for ammonium thioglycolate.

RESULTS AND DISCUSSION

EXTENSIONAL PERMANENT SET

Linear viscoelasticity about the set in extensional permanent treatment served as the basis for the prediction of the bending set and wave efficacy. The validity of this approach was confirmed by the agreement between the observed set values (Sℓ) and the calculated set values (So) obtained using the equation shown below derived by Wortmann (4), which is based on Denby's linear viscoelasticity theory (8).

$$So = (1 - Ere/Ero) \times 100\ (\%), \tag{5}$$

where Ere is the normalized residual stress after reoxidation (Fre/Fo) and Ero is the normalized Young's modulus after reoxidation (f/Fo).

All data derived from the extensional experiments using the wave lotions listed in Table I are presented in Table II. In addition, Figure 4 shows a graph of the calculated values (So) plotted vs. the observed set (Sℓ) values taken from Table II. The experiments were performed under two conditions. In the first group (Exp No. 1–9 in Table II), all wave lotions listed in Table I were applied for a reducing time of 14–19 min. In the second group (Exp No. 10–18 in Table II), only the neutral strength wave lotion from manufacturer A (A–N) was applied for various reducing times (1–12 min). The plots shown in Figure 4 pass through the origin and closely follow a straight line with a slope of 1.00, correlation factor $r = 0.997$. These results therefore indicate that the hair fibers exhibited linear viscoelastic behavior about the set. Jeong (9) reported similar results for wool fibers.

However, Wortmann obtained very different results under his experimental conditions, which while being similar to those used in the present study, were different in three important aspects, as described in the Experimental section. Specifically, Wortmann reported that the observed set values (Sℓ) were much smaller than the calculated values (So) (4). However, the reasons for the difference in values remain unclear at this time and further experiments are required to be conducted to verify the reason for this difference.

Table II
Extensional Permanent Waving Set

Exp No	Sample	*t* (min)	Pa (%)	Ere (%)	Ero (%)	ℓ(mm)	△ℓ(m)	Sm(%)	So(%)
1	A–S	16.7	90.5	3.8	58.2	69.0	65.7	95.2	93.5
2	A–N	15.2	79.9	15.5	79.1	67.5	54.8	81.2	80.4
3	A–W	16.2	67.7	29.8	83.0	67.8	44.3	65.3	64.1
4	B–S	17.2	88.1	4.7	61.7	69.0	65.2	94.5	92.4
5	B–N	15.2	82.2	11.2	75.1	68.4	58.6	85.7	85.1
6	B–W	19.2	72.7	23.6	82.6	68.5	49.6	72.4	71.4
7	C–S	17.3	85.6	8.8	71.2	68.4	59.0	86.3	87.6
8	C–N	16.1	58.5	38.8	85.3	67.9	37.0	54.7	54.5
9	C–W	14.3	40.9	56.5	83.6	67.8	22.1	32.6	32.4
10	A–N	1.3	21.2	75.2	91.3	68.6	10.6	15.5	17.6
11	A–N	2.6	29.3	66.3	90.6	67.9	16.7	24.6	26.8
11	A–N	3.5	42.5	53.0	87.7	67.9	25.0	36.8	39.6
12	A–N	4.3	40.0	54.3	86.0	67.3	24.3	36.1	36.9
13	A–N	5.0	45.3	48.6	85.4	66.5	27.4	41.2	43.1
14	A–N	6.0	64.9	29.6	82.8	67.5	42.7	63.3	64.3
15	A–N	7.5	67.1	28.7	83.4	67.4	43.3	64.2	65.6
16	A–N	9.0	72.4	22.4	82.3	68.4	48.0	70.2	72.8
17	A–N	10.2	60.0	36.4	84.9	67.4	38.2	56.8	57.1
18	A–N	11.8	70.2	26.7	82.5	67.8	45.8	67.6	67.6

t (min), reduction time (see step 2 in Fig. 2); Pa (%), apparent progress of reduction (see equation (2) and step 2 in Fig. 2);Ere (%); normalized residual stress after reoxidation (see step 5 in Fig. 2); Ero (%); normalized Young's modulus after reoxidation (see step 7 in Fig. 2); ℓ (mm); extended length measured on recording paper (see step 6 in Fig. 2); Δℓ (mm), set length measured on recording paper, (see step 6 in Fig. 2); Sℓ, observed set [see equation (1)]; So, calculated set using equation (5).

Homogeneity of the hair fiber microstructure. Wortmann reported that the disagreement between the So and Sℓ values was significant and assumed that it was due to inhomogeneity of the radial distribution of the modulus in the hair fiber. He confirmed this assumption by performing a bending test independent of the extensional test (10). Because of the good agreement of the So and Sℓ values in the present study, the inhomogeneity of the radial distribution of the modulus in the hair fibers as proposed by Wortmann were not considered in the present study.

Characterization of the wave lotions. The set of a permanent wave is governed mainly by the reduction process, which is determined by the characteristics of the given wave lotion.

In Japan, wave lotions have been qualitatively characterized by their strength in wave molding of the hair: S (strong), N (neutral), and W (weak). As a result, it is impossible to objectively assess the differences in the holding characteristics of wave lotions produced by different manufacturers. The use of Pa/*t* curves resolves this problem, because the curves illustrate the progress of reduction with time, and the differences in the various waving lotions can be identified by comparing the corresponding curves.

Figure 5 shows the Pa/*t* curves for the wave lotions listed in Table I, with parts presenting the curves for the waving lotions produced by manufacturers A, B, and C, respectively.

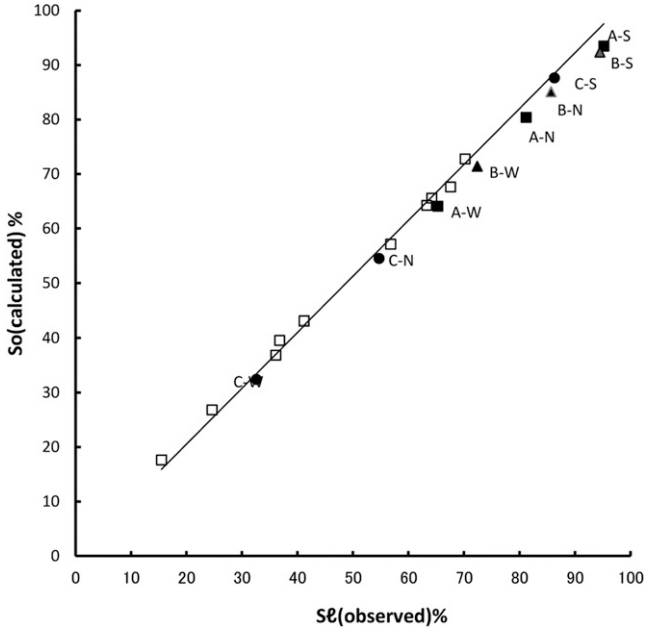

Figure 4. Relationship between the observed set (Sℓ) and the calculated set (So) obtained using equation (5). The letter for each plot indicates the sample name (see Table I); (■), (▲), and (●) indicate the applied reduction times shown in Exp. Nos.1–9 in Table II. A–N applied for the various reduction times are listed in Exp. Nos. 10–18 in Table II. Correlation: $y = 1.00X$, $r = 0.997$. Note: Linear viscoelasticity about set in extensional permanent treatment.

The holding strengths (S, N, and W) of the lotions from each manufacturer agreed well with the order of the corresponding Pa values obtained at 15 min. If the user applies wave lotions produced only by one manufacturer, the Pa/*t* curves may not be significant, because the order of the holding strengths (S, N, and W) agreed with the Pa values obtained at 15 min, and they are not necessary for selecting a particular wave lotion. However, without the Pa/*t*, the characteristic behavior of B–N, would not be detected, i.e., intersection of B–N and B–S [see Manufacturer B in Figure 5(A)]. In addition, comparison of the behavior of wave lotions of the same strength (S, N, or W) from different manufacturers is not possible when only on the basis of the indication of S, N, or W on the package. In these cases, Pa/*t* curves provide helpful information, as can be seen in Figure 5(B). The differences in the curves were found to be significant (p value < 0.05) as determined using a two-way layout analysis of the variance for six repeated test results for each lotion.

Therefore, for practical purposes, an indication of the strength of the wave lotion (S, N, or W) as a numeric expression, such as the Pa value at 5 min taken from the Pa/*t* curve (see Practical assessment of wave efficacy for an explanation of the use of 5 min) is desired. However, in order to provide Pa values at 5 min that can be compared, a standard apparatus and method for determining the Pa/*t* curves of permanent waving lotions is needed.

Note that the intersection of the B–S and B–N curves shown in Figure 5(A) can only be detected by plotting the Pa/*t* curves. In this case, the Pa values for the B–N lotion were greater than those of the B–S lotion at a short reduction time (5 min) and less than those of the B–S lotion at a long reduction time (15 min). This reversal of the reduction behavior is

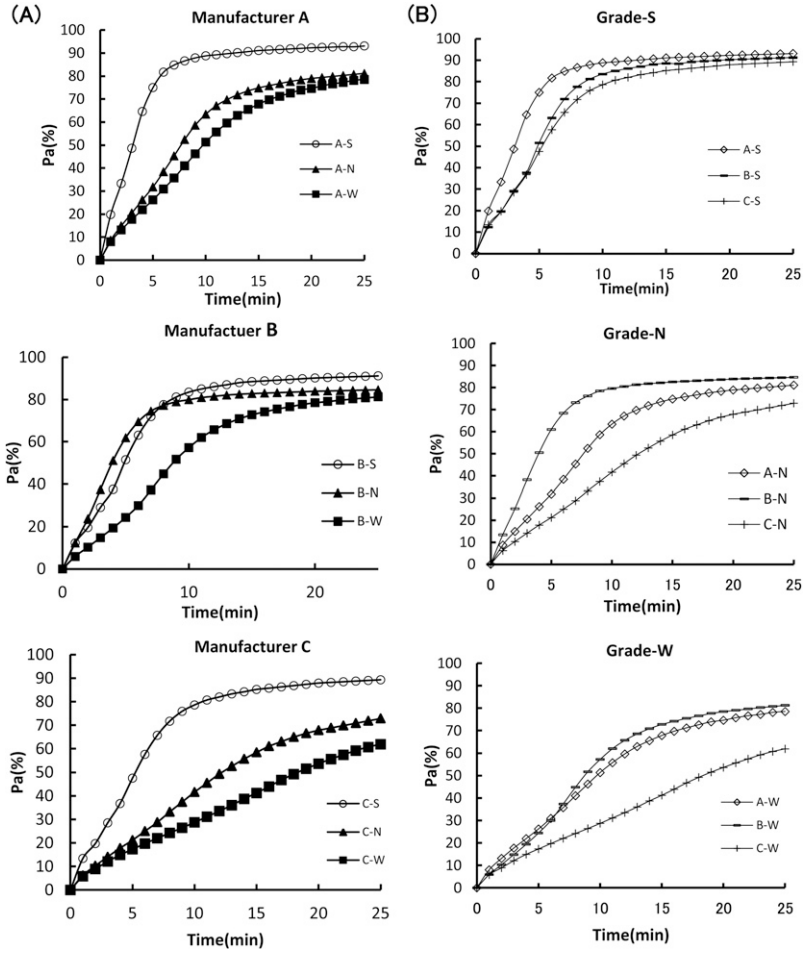

Figure 5. Pa/*t* curves for different wave lotions from representative manufacturers. (A) Comparison of Pa/*t* curves for products from manufacturers A, B, and C. (B) Comparison of Pa/*t* curves for the same grades of products from manufacturers A, B, and C. Note: The intersection of the B–S and B–N curves in (A) (see text).

discussed in the following sections on the bending set and wave efficacy (see Bending permanent set and Practical assessment of wave efficacy). Most importantly, the Pa/*t* curves were used to analyze the results for the various wave lotions investigated in this study.

Characteristic reduction kinetics for the treatment of hair with the NH_4 salt of thioglycolic acid. Reviewing shapes of Pa/*t* curves in Figure 5, a question arose whether reduction kinetics of ammonium thioglycolate (TGA-NH_4) was the same as that of sodium thioglycolate (TGA-Na) presented by Wickett (11), though the study by Manuszak (12) followed Wickett's conclusion about TGA-Na, and Wortmann (4) cited the same for interpreting his theory.

However, the present study was focused on the characterization of the set of different wave lotions rather than the reduction kinetics, Pa/*t* curves were obtained for direct reduction without any pretreatment to remove the physical relaxation of the hair prior to reduction, as was performed in previous studies conducted by Wickett (11) and Manuszak

(12). However, approximate determination of the reduction kinetics in hair was performed without pretreatment in order to confirm that reduction kinetics of TGA-Na follows pseudo first-order reaction and in this way compared with that of TGA-NH_4 solutions. Both solutions were 0.6 M in thioglycolic acid and adjusted to a pH of 8.6 (see Preparation of sodium and ammonium thioglycolate solution in Experimental section).

As can be seen in Figure 6(A), Wickett's results for TGA-Na were approximately reproduced using our simplified conditions, although slight deviations were observed during the initial 6 min. In addition, it was found that the reduction proceeded much more rapidly with TGA-NH_4 than with TGA-Na. Furthermore, the –ln (Ft/Fo) vs. time plot for of TGA-NH_4 yielded a straight line for the initial 10 min but then deviated from a straight line thereafter. These results suggest that reduction using TGA-NH_4 follows a pseudo first-order reaction during the initial stage; however, beyond this stage, the mechanism of reduction is no longer the same. Notably, despite the fact that the results were

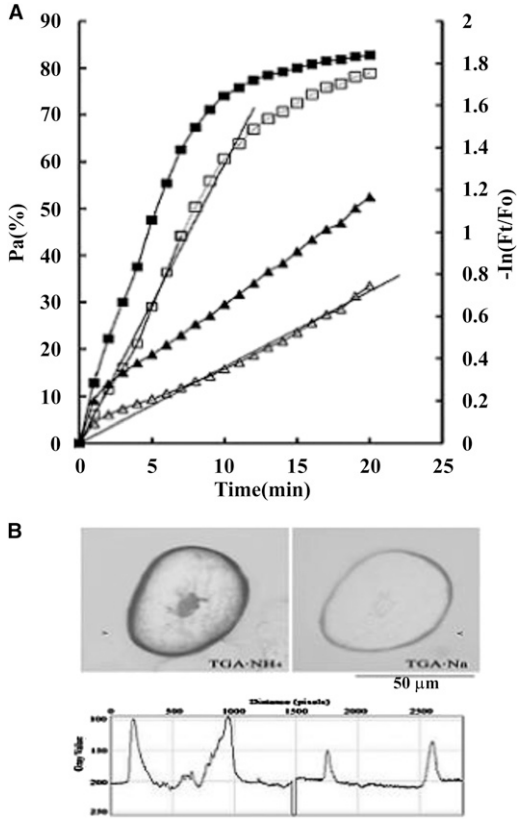

Figure 6. Comparison of the reduction kinetics for the Na and NH_4 salts of thioglycolic acid: Pa and –ln(Ft/Fo) vs. time. (A) Left axis: Pa/*t* curves for (▲) TGA–Na and (■)TGA–NH_4; right axis: –ln(Ft/Fo) for (△) TGA–Na and (□) TGA–NH_4 vs. time; TGA–Na (△) vs. time: $y = 0.036X$, $r = 0.992$ and TGA–NH_4(□)vs. time: $y = 0.13X$, $r = 0.989$ only during the initial stage. Conditions; salt concentration: 0.6 M; pH: 8.6. Note: the plot of –ln(Ft/Fo) for TGA–NH_4 vs. time also shows a linear relationship only in the initial stage of the reaction. (B) Optical microscopic images of the sections of white hair pretreated with NH_4^+ and Na salts of thioglycolic acid and stained with methylene blue. Bottom: Gray-scale image obtained by scanning along the line between the two points indicated by arrowheads on the micrographs (taken by Dr. Kawamura).

obtained at a pH of <9, the results for TGA-NH_4 disagreed with both Wickett's conclusion (11) that TGA-Na kinetics are pseudo first-order at pH 9 or below. Considering all of the above data, it can be concluded that the reduction kinetics for TGA-NH_4 in hair is different than those for TGA-Na.

Next, the reduction characteristics for all TGA-NH_4 wave lotions listed in Table I were evaluated and found to be similar to those described above. However, the plots of –ln(Ft/Fo) for the C–N and C–W lotions, which are very weak wave lotions, vs. time appeared to follow pseudo first-order kinetics, as can be seen in Figure 7(A). To determine whether the behavior observed in these plots for the C–N and C–W lotions only occurred in the initial stages of the reactions, the reduction time was increased from 20 to 90 min. Figure 7(B) shows the Pa/*t* curve and plot of –ln(Ft/Fo) vs. time for the C–W wave lotion over an extended period of time (90 min). It can be clearly seen that the plot of –ln(Ft/Fo) vs. time for the first 20 min in Figure 7(B) corresponds to the initial stage of the reduction,

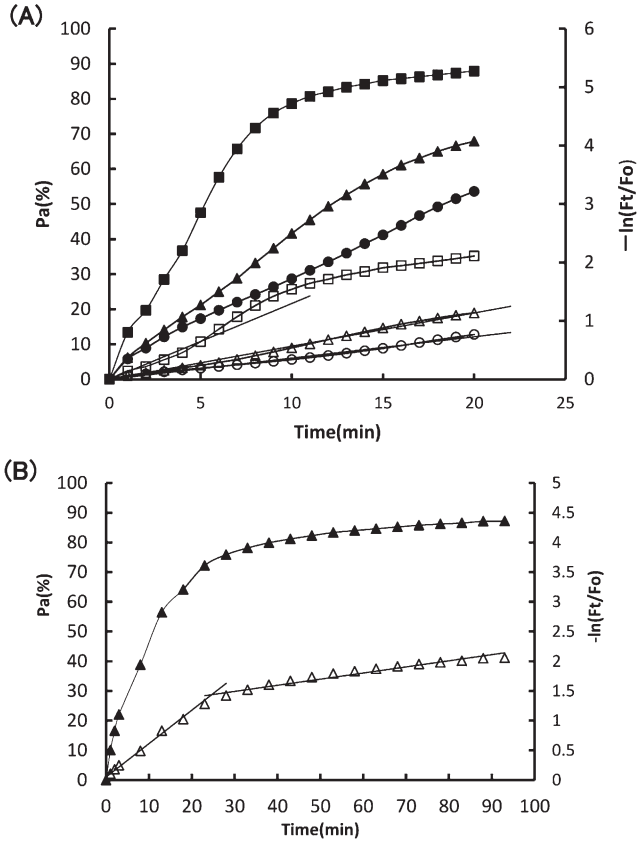

Figure 7. Characteristics of the reduction kinetics of TGA–NH_4 wave lotions. (A) Left axis: Pa vs. time for (■) C–S, (▲) C–N, and (●) C–W; Right axis: –ln(Ft/Fo) vs. time for (□) C–S *:y* = 0.136X, *r* = 0.992 (only initial stage), (△) C–N *:y* = 0.057X, *r* = 0.996, and (○)C–W: *y* = 0.36*X*, *r* = 0.996. Note: The results for C–N and C–W (weak wave lotions) suggest that these reactions were pseudo first order. (B) Left axis: At an extended reduction duration of 90 min, (▲) Pa vs. time for C–W; right axis: (△)–ln (Ft/Fo) for the same. Note: This reaction exhibited the same pattern as other TGA–NH_4 .

because the slope of the line changed dramatically for reduction times greater than 20 min. These results therefore confirmed that reductions with the NH_4^+ salts listed in Table I follow pseudo first-order kinetics only during the initial stage of the reaction, and beyond this stage, the reductions proceeded by a different mechanism.

DIFFUSION RATE OF TGA-NA AND TGA-NH_4

Two main factors may contribute to the differences in the reduction kinetics for the Na^+ and NH_4^+ salts: the dissociation constants $K_2 = [H^+][^-S\text{-}CH_2\text{-}C00^-]/[HS\text{-}CH_2\text{-}C00^-]$ for TGA-Na and TGA-NH_4 and the difference in their diffusion rates into hair fibers. The K_2 values for TGA-Na and TGA-NH_4 have been determined using titration and spectrometric methods (13,14); however, no difference was detected. With respect to their diffusion rates into hair, Garcia et al. (15) found that using the differential extension method, TGA-NH_4 rapidly diffuses into hair by the differential extension method. In the present study, the rates of diffusion of TGA-Na and TGA-NH_4 were compared using the method described in part 5 of the Experimental section.

Figure 6(B) shows the microphotographs of the obtained dyed cross sections along with plots of the gray values of the digital images (bottom). It can be concluded from the figure that the diffusion of TGA-NH_4 was much faster than that of TGA-Na. Therefore, because both reductions followed a pseudo first-order reaction for the initial 5 min, the large difference in the performance of the NH_4 and Na salts can be attributed to their different diffusion rates.

The diffusion patterns of TGA-NH_4 and cysteine into hair were studied by Kuzuhara and Hori using a combination of microspectrophotometry and dyeing techniques (16). These researchers found that the different patterns for diffusion result from the electrostatic interaction of the free amino groups of cysteine with the anionic ions of human hair. However, it was not possible in the present study to explain the mechanisms underlying the different diffusion rates for TGA-NH_4 and TGA-Na. On the basis of the available information, it is thought that the interactions between the NH_4^+ and Na^+ groups associated with thioglycolic acid and the anions on the surface of human hair may be quite different. Further study is needed to elucidate the actual cause of the different diffusion rates.

It was demonstrated, however, that the reduction kinetics for TGA-NH_4 was different from that of TGA-Na, and thus the conclusions on the kinetics of TGA-Na drawn by Wickett cannot be generally expanded to the ammonium salt of thioglycolic acid.

BENDING PERMANENT SET

The subject of this experiment was the correlation between the bending and extensional sets. The same single fiber was divided into two pieces, 10 cm and 15 cm in length. The shorter fiber was used for the bending test and placed in the apparatus shown in Figure 3. The longer fiber was used for the extensional test as described above. The waving lotions A–S, A–N, B–S, B–N, and C–W were selected as the representative wave lotions for this investigation, and each was applied for various reduction times. The results are presented in Table III and Figure 8(A), which show the relationship between the experimentally determined set values for the bending and extensional treatments. The bending sets correlated well with the

Table III
Bending and Extensional Setting Tests Using the Same Hair

Exp. No	Wave lotion	Time (min)[a]	Pa(%)	Sℓ(ext)(%)[b]	Sℓ(bend)(%)[c]
1	A–S	9.5	80.3	84.3	7.9.0
2	A–S	11.1	80.8	86.3	84.3
3	A–S	15.0	84.8	89.4	82.6
4	A–N	10.0	52.9	49.5	58.8
5	A–N	9.2	48.4	51.9	51.8
6	A–N	15.4	67.5	65.1	66.1
7	A–N	15.1	64.3	67.1	71.5
8	A–N	15	62.3	60.4	61.0
9	B–S	16	56.3	87.4	80.0
10	B–N	16.3	69.1	78.3	73.0
11	B–S	5.0	87.4	56.3	56.8
12	B–N	5.0	78.3	69.1	68.0
13	C–S	3.4	20.4	21.1	34.5
14	C–S	4.7	27.6	27.6	41.3
15	C–S	10.0	36.4	35.4	46.7
16	C–S	10.6	43.4	42.2	52.7
17	C–S	9.3	68	70	70.0
18	C–S	14.2	72.5	74.6	83.3
19	C–S	11.9	72.9	76.8	77.5
20	C–S	10.1	40	39.6	47.3
21	C–S	5.0	26.7	24.7	37.9
22	C–S	15	51.8	53.8	53.0
23	C–S	9.1	63.2	64.1	65.8

[a]Reduction time.
[b]Extensional set [equation (1)].
[c]Bending set [equation (3)].

extensional sets (y = 0.787x + 18.20, r =0.974). Notably, after 5 min of reduction, the bending set value for the B–N lotion was greater than that of the B–S lotion, while it was less than that of the B–S lotion after 16 min of reduction. This reversal is similar to the results obtained for the Pa/t curves for B–S and B–N lotions, as shown in Figure 5(A), and suggests that the mechanism of deformation is the same for both bending and extensional treatments.

Furthermore, these results demonstrate that the bending set behavior can be accurately predicted by the extensional set behavior, which is in disagreement with Wortmann's claim regarding the weak correlation between the extensional and bending sets.

Larger bending sets than extensional sets.

One problem associated with the results given in Figure 8(A) is that the bending sets are larger than those obtained after extensional treatment, because the straight line shown in the figure does not pass through the origin. The issue of larger bending sets compared to the corresponding extensional sets has been discussed by Wortmann (10) and Feughelman

(17) on the basis of their respective theories. However, from a macroscopic view point, the simplest explanation is that during bending treatment, the exterior surface of the fiber is extended, while the interior surface of the fiber, which is in contact with the cylinder, is compressed; consequently, diffusion of the reducing agent on the exterior surface occurs more rapidly than on the interior surface.

Thus, to verify the effect of extension and compression on the rate of diffusion and reduction on the exterior and interior surfaces, the following experiment was conducted. A single hair fiber fixed in the device shown in Figure 3 was reduced for 5 min using the C–S wave lotion, rinsed with water, and then soaked in 0.1 M $HgCl_2$ for 10 min (18). The distribution of the Hg formed as S–Hg–S bonds was then determined using the method described in Determination of the distribution of Hg (in Formed S–Hg–S Bonds) in hair of the Experimental section.

Figure 8(B) shows the relationship between the Hg L-line count and the 44 measurement locations. The integrated Hg count at the outside edge of the fiber was much larger than that at the inside edge, and the extent of Hg diffusion at the outside edge was greater than that at the inside edge. These results indicate that the effect of diffusion at the outside edge was greater than that at the inside edge, and thus a greater effect is expected for the bending treatment than the extensional treatment.

PRACTICAL ASSESSMENT OF WAVE EFFICACY

The practical wave efficacy assessment results provided by the professional hairdresser are presented in Figure 9(A) (copyright provided to us by H. Takahara). In the hairdresser's report, it was emphasized that the wave efficacy of the B–N wave lotion was greater than that of the B–S lotion, even though –S wave lotions usually have greater strength than –N lotions. This comment provides significant validation of the proposed approach. The practical assessment that the wave efficacy of the B–N lotion was greater than that of the B–S lotion corresponds with the difference in the Pa values taken from the respective Pa/*t* curves for the B–S and B–N lotions at 5 min. In addition, a comparison of the reducing condition used for the extensional and practical treatments revealed that the volume of the reducing agent relative to the volume of hair was practically infinite for the extensional treatments, but on the order of 1–2 for the practical treatments. Therefore, reduction for 15 min during the extensional treatment is clearly too severe, and the values for Sℓ (ext) on the Pa/*t* curves at a reduction time of 5 min should correlate well with the wave efficacy expected during practical applications.

Figure 9(B) shows the average practical assessment values for the wave efficacy plotted against the Sl(ext) values taken from the Pa/*t* curves in Figure 9(C) (prepared using the data in Table II) at 5 min for each wave lotion listed in Table I. These results suggest that the wave efficacy can be predicted using the Sl(ext) value.

Accuracy of wave efficacy prediction. Although there is a correlation between the wave efficacy results and the extensional set values, it is lower than that between the wave efficacy and the bending set values (wave efficacy vs. Sℓ: $y = 0.263X + 42.491$, $r = 0.911$). In addition, the order of the values for each wave efficacy did not exactly coincide with that of the Sl(ext) values, as can be seen in Table IV. Therefore, it is necessary to increase the number of wave efficacy tests and analyze them statistically to achieve more accurate predictions.

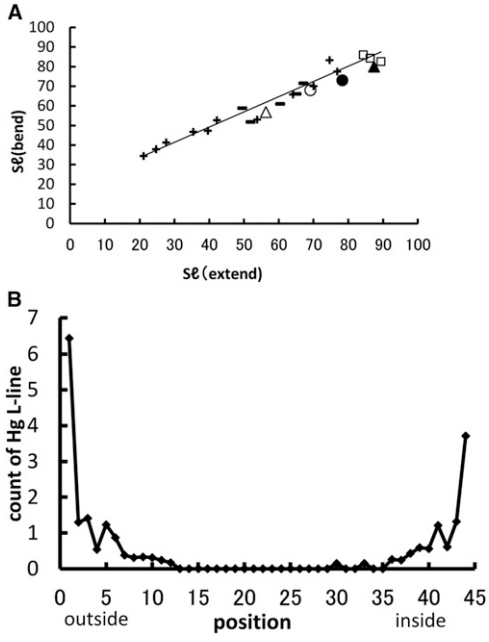

Figure 8. Relationship between the extensional set and the bending set. (A) Plot of Sℓ(bend) vs. Sℓ(ext) using the same hair under the various conditions shown in Table III. (□)A–S (reduction time 9.5–11 min); (–) A–N (9–15 min);((+) C–W (3–15 min).B–S (5 min); (●)B–N (16 min); (○) B–N: (5 min); (▲) B–S (16 min); (△)B–S (5 min) Correlation: $y = 0.787X + 18.20$, $r = 0.974$. Note: In short reduction time (5 min), (○)B–N > (△) B–S, in long reduction time (16 min) (●)B–N < (▲)B–S. This behavior is similar to that observed for the Pa/t curves of B–N and B–S as shown in Figure 5(A). (B) Difference in the reduction rates in the exterior and interior of wound hair using TGA–NH_4 is determined on the basis of the formation of S–Hg–S bonds. The exterior reduction is clearly greater (see text).

HAIR DAMAGE

Hair damage after permanent treatment, such as changes in appearance, roughness, gloss, and stiffness, are evaluated by hairdressers using a feeling test. Such delicate

Table IV
Wave Efficacy and Setting at 5 Min on Pa/t Curve

Wave lotion	Pa at 5 min(%)	Calc.Sℓ(ext)(%)[a]	Wave efficacy(%)[b]
	Average (SD)	Average Sℓ	Average (±)
A–S	75 (4.2)	75.2	58.2 (±2.5)
A–N	31.8 (5.6)	25.2	49.7 (±2.5)
A–W	26.2 (6.1)	18.7	45.7 ± 2.5
B–S	51.5 (9.1)	48.0	59.2 (±2.5)
B–N	61 (11.3)	59.0	61.2 (±2.5)
B–W	24.4 (1.5)	16.6	48.8 (±2.5)
C–S	47.5 (9.5)	43.4	51.5 (±2.5)
C–N	21.2 (3.7)	12.9	45.5 (±2.5)
C–W	17.3 (1.9)	8.4	42.5 (±2.5)

[a]Calculated using the graph in Figure 9(C).
[b]Measured by a hairdresser.

Table V
20% Index of Virgin Hair in Water at 30°C

Japanese senior high school girls[a]			Japanese in beauty parlor[b]		Chinese[c]	German ladies[d]
	(45)		Parlor-A(8)	Parlor-B(7)	(6)	(8)
61.2	61.0	61.7	61.5	62.2	62.4	62.4
60.7	60.2	62.1	61.1	61.4	61.7	59.1
61.0	62.5	61.9	61.1	61.3	59.6	60.7
62.5	60.9	62.3	61.6	61.7	61.1	61.4
60.4	59.9	60.5	61.9	62.0	61.3	61.2
62.0	62.8	63.4	61.7	61.1	60.2	60.5
60.4	60.9	62.2	61.4	62.5		61.6
61.8	62.0	62.6	62.2			
62.5	62.6	61.8				
61.7	62.6	62.6				
61.7	62.1	61.3				
61.2	62.1	62.9				
61.5	61.8	61.4				
61.9	60.2	62.5				
62.1	61.2	61.9				
Average of 20% index (%)		61.7	61.6	61.7	61.1	61.0
			The total number of virgin hairs, 74		Mean ± SD = 61.6	±0.8(SD)

[a]Donated by students at Tokyo Metropolitan Toyama High School, Tokyo, Japan.
[b]From Parlor A (the beauty parlor "Boy" in Tokyo) or Parlor B (the beauty parlor "ADOMI" in Hachinohe).
[c]Picked up at random from Chinese hair tissue purchased from hair supplier (Deaulax Co. Ltd., Saitama, Japan).
[d]Donated by Dr. S. Roeper in Hamburg, Germany.

characteristics cannot be determined using mechanical tests. However, if damage is restricted to a decrease in the stiffness or the Young's modulus after treatment, damage evaluation should be possible by measuring Ero (f/Fo), as previously discussed.

Ero is directly related to the set value as shown in equation (5) and it should be emphasized that in the present study Ero did not simply decrease when Pa increased but abruptly decreased when Pa was approximately 80%, regardless of the wave lotion and the reduction time, as shown in Figure 10(A), which was drawn by plotting the values for Ero vs. the values for Pa listed in Table II. However, these plots with steep declines were obtained only at long reduction times. In order to confirm this important behavior, therefore, Ero was measured at various Pa values for the A–S, A–N, and C–W lotions as representative wave lotions. As can be seen in Figure 10(B), the abrupt decrease in Ero when Pa was ~80% was observed for the three wave lotions. It should be noted that the existence of this critical point (Pa = 80%) reflects the point at which hair damage occurs. In addition, it can be imagined that this behavior relates with the characteristic kinetics of TGA-NH_4

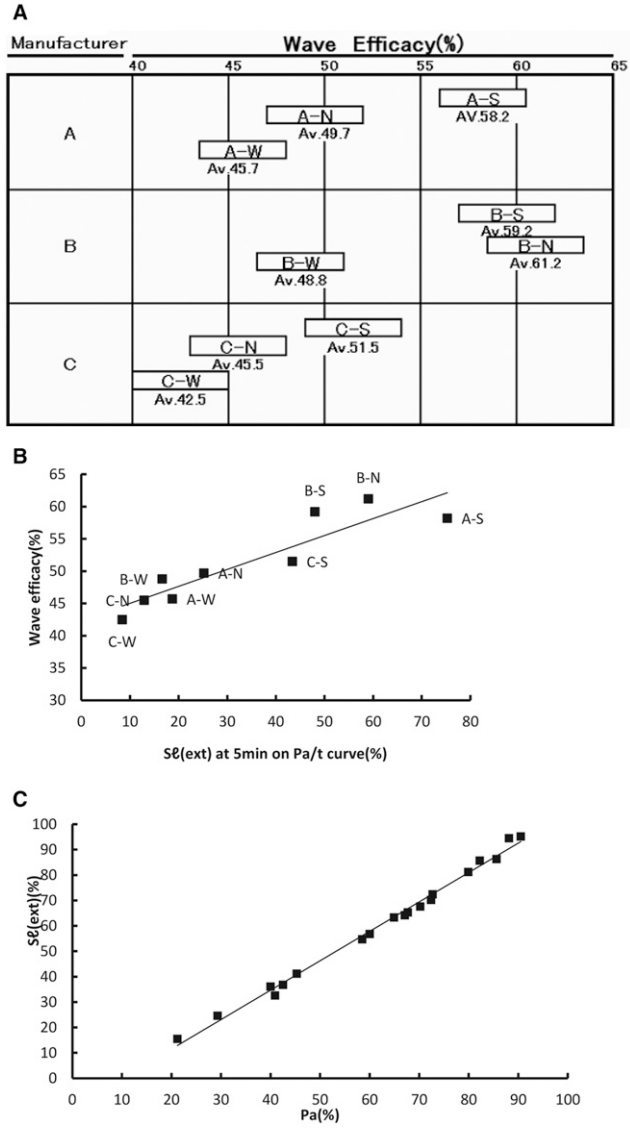

Figure 9. Relationship between the wave efficacy measured by a hairdresser and the set in an extensional permanent treatment. (A) Wave efficacy map reported by a hairdresser. (B) Relationship between the wave efficacy and the set Sℓ(ext) at 5 min on the Pa/*t* curves for each wave lotion (See Table IV); correlation: $y = 0.263X + 42.491$, $r = 0.911$. (C) Relationship between Pa and the observed set(l) values listed in Table II for the determination of the Sl values shown in (B); correlation: $y = 1.158X - 11.662$, $r = 0.996$.

described in Characteristic reduction kinetics for the treatment of hair with the NH_4 salt of thioglycolic acid. Figure 10 (p. 22).

While Ero (f/Fo) can be measured in the laboratory, it is impossible to determine a customer's Fo, i.e., the Young's modulus of the customer's virgin hair, in a beauty parlor.

Fortunately, it was also found in the present study that the 20% index values in water at 30°C for all individual virgin hair samples remained constant at 61.6 ± 0.8%, as shown in

Table VI
Experiment for Estimating Hair Damage (Ero) by 20% Index

Exp.No	Wave lotion	Hair	Pa(%)	Ero (%)	20% Index (%)
0	—	Virgin	0	100	61.6 (Av.)
1	A–S	Standard	26.5	92.9	59.9
2	A–S	School girl-1	31	91.6	59.2
3	A–N	School girl-2	40.3	86.7	57.7
4	A–S	Standard	61.1	90	57.4
5	A–S	Standard	71.2	81.8	56.4
6	C–W	School girl-3	84.9	79.2	56.1
7	A–S	Standard	77.1	73.1	56.9
8	A–S	Standard	80.1	71.5	55.1
9	A–S	Standard	87	64.6	58.8
10	A–S	Standard	90	50.4	61.2
11	A–S	Standard	91.4	49.9	62.9
12	A–S	Standard	91.4	39.6	63.6
13	A–S	Standard	95.8	30.8	66.6
14	A–S	Standard	93.7	28.5	66.3
15	A–S × 4 times	Standard	84.5	25.8	63
16	A–N × 4 times	Standard	76.6	50.3	57.1

[a]Standard: donated by beauty parlor "BOY": school girls (-1, -2, and -3) were picked hairs donated from Tokyo Metropolitan Toyama High school, Tokyo, Japan.

Table V. Since it was found that all the virgin hairs show the constant 20% index value in water at 30°C, it is expected that to estimate hair damage (Ero) by measuring only 20% index of the given hairs, if there is a correlation between 20% index and Ero. To determine the effect of perm treatment on the Ero(100%) and 20% index (61.6%) values, Ero(100%) and 20% index (61.6%) for the same virgin hair sample were measured during extensional permanent treatment under three conditions of different virgin hair samples, three types of wave lotions (A–S, A–N, and S–W), and various reduction times. The results are presented in Table VI and Figure 11, which show the plot of the 20% index values against the Ero values. Notably, the 20% index values fell on the line H when the Ero values were above 80%. However, for Ero values less than 80%, the 20% index values for the abruptly increased following line L, forming a V shape. As importantly, the graph shown in Figure 11 can be generally applied for anyone whose Fo is unknown.

However, it must be noted that this figure has a significant weak point, because the H and L lines were obtained with virgin hair that was treated for the first time. Accordingly, these lines cannot be directly applied for hair that has been repeatedly treated, such as is the case for most customers that visit beauty parlors. Therefore, to predict hair damage after repeated permanent treatments, line R was obtained by plotting the 20% index values vs. Ero after repeating the treatment four times (5 min of reduction corresponds to the reduction time of a practical treatment; see Practical assessment of wave efficacy on wave efficacy) using wave lotions A–S and A–N. Line R shifted to the left of line L by approximately 20%, indicating that severe damage results owing to repetitive treatment.

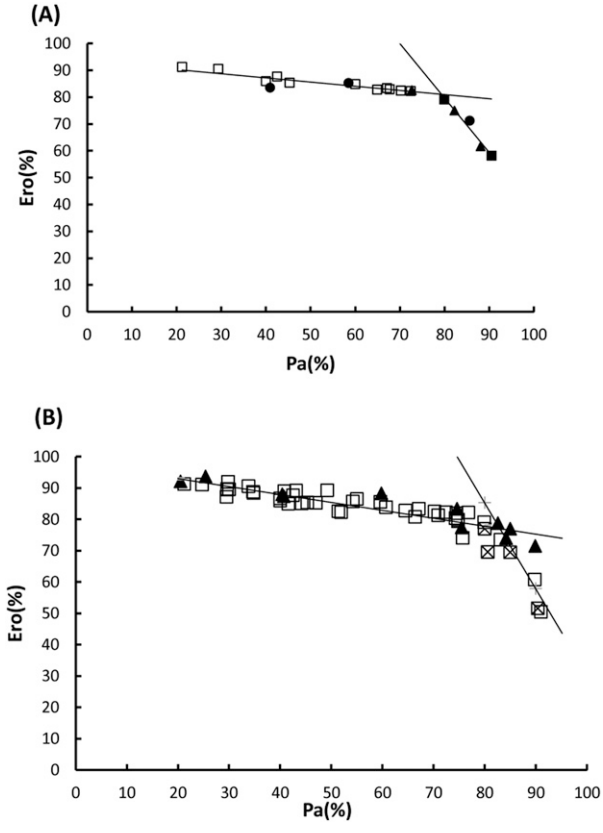

Figure 10. Relationship between Pa and hair damage (Ero) (abrupt decrease in Ero). (A) Plot of Pa vs. Ero using the values listed in Table II. The symbols are the same as those in Figure 4. Note: An abrupt decrease in the Ero value is observed at Pa = 80%. (B) Confirmation of the results shown in (A) using the A–S, A–N, and C–W lotions: (□), A–S; (×), A–N; and (▲), C–W. Note: The results shown in (**A**) are reproducible for the different types of wave lotions from different grade and manufacturers.

On the other hand, the shape of the hysteresis curves changed in the order H then L then R, as shown in Figures 12(B), 12(C), and 12(D), respectively. Figure 12(A) shows the hysteresis curve for the virgin hair. The curve for line H marked with an arrow has an obvious shoulder, while that for line L has much less of a shoulder, and that for line R is even smoother. However, although the differences in the curvatures of the curves for L and R appear to be small as observed by the eye, geometric measurement of the curvatures revealed values of 0.76×10^{-2}, 7.1×10^{-2}, 4.3×10^{-2}, and 3.1×10^{-2} for the curves for the virgin hair, and lines H, L, and R, respectively.

Accordingly, the use of the graph shown in Figure 11 for estimation of hair damage is limited. The graph can only be directly applied for virgin hair that is to be treated for the first time. To estimate the damage to hair that has received repeated permanent treatments, it is possible to approximately estimate the damage to a customer's hair. If the 20% index value is >61.6% and a line R hysteresis curve is obtained, hard damage (Ero << 50%) can be expected. If the 20% index value is <61.6% and a line H hysteresis curve is obtained, then low damage (Ero > 80%) can be expected. On the other hand, if the

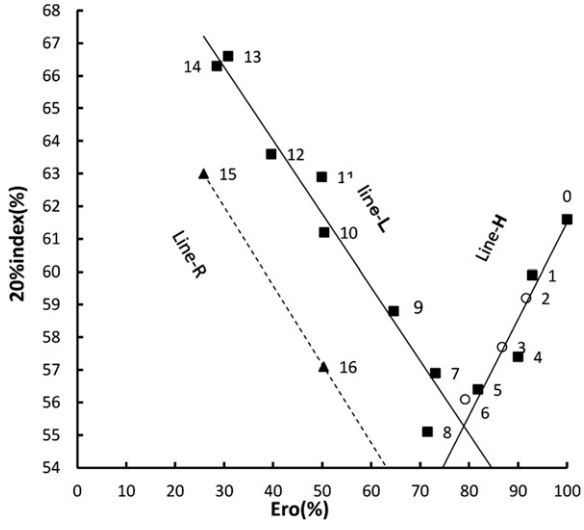

Figure 11. Estimation of hair damage (Ero) using the 20% index. Plot of Ero vs. the 20% index values listed in Table VI (the number affixed to each plot indicates the Exp. No. in Table VI). With increasing hair damage, the 20% index decreased up to Ero = 80% along line H and then increased along line L forming a V shape. Line R: results for four repeated permanent treatments. Note: The 20% index value for virgin hair was constant in water at 30 °C (See Table V).

20% index value is <61.6% and a line L or R hysteresis curve is obtained, medium to hard damage (Ero < 50%) can be expected.

Summarizing the above, only the 20% index value can be used to estimate hair damage if virgin hair is to be treated, but it is insufficient for estimating the damage to hair that has previously been repeatedly permed. The relationship between the values for Ero and the 20% index for repeated permanent treatments must be further investigated.

Mechanism of the abrupt decrease in Ero at Pa = 80%. We speculate that the steep decrease in the value of Ero can be interpreted by the two-phase concept (19); hair fiber consists of continuous linear and elastic filaments (phase C) embedded in an amorphous matrix (phase M). To substantiate whether the steep decrease in Ero is related to only phase C or both phases C and M, both values for Ero and the 20% index were obtained for various values of Pa using the same hair fiber, because the large increase in the 20% index value at Pa = 80% might be related with the abrupt variation in the value of Ero. As can be seen in Figure 13, a steep increase in the 20% value coincided with a rapid decrease in the value of Ero at approximately Pa = 80%. These results indicate that the steep decrease in Ero is related not only to phase C but also to phase M, because a steep increase in the 20% index indicates initiation of entanglement of the filaments in the microstructure of the hair.

This entanglement of the filaments in phase C and M occurs by disorganization of the microstructure of hair, then the filaments in both phases are liberated from the originally restrictive structure loosened and entangled.

Consequently, the locations of SH residues produced in the crystalline filaments are no longer located near one another where they can be readily reoxidized using an aqueous

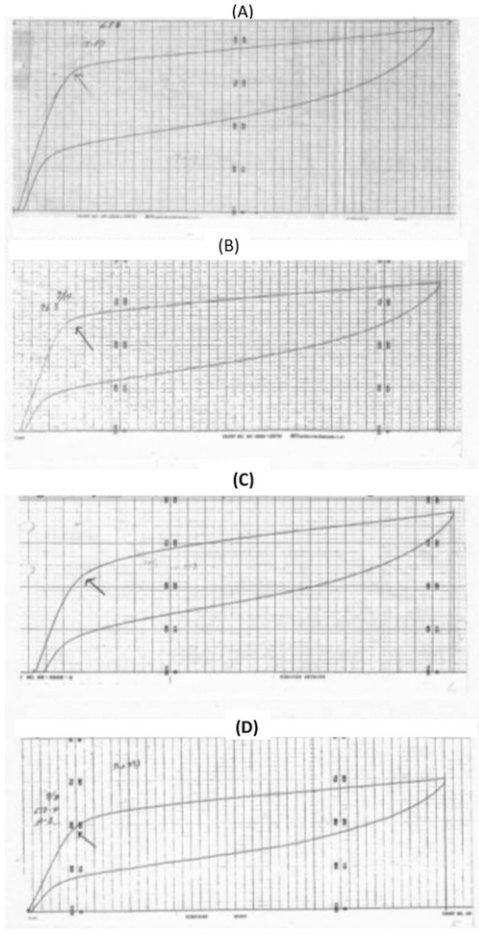

Figure 12. Changes in the hysteresis curves with an increase in hair damage. Hysteresis curves obtained for the 20% index values (A),(B),(C), and (D) were determined under the conditions listed in Table VI (Exp. Nos. 0, 3, 9, and 16). (A) Virgin hair, (B) a little damaged hair (on line H), (C) hard damaged hair (on line L), and (D) hard damaged hair by repeated treatments (on line R). Note: The curvatures indicated with arrows decreased as the hair damage increased.

0.03g/100g H_2O_2 solution (21). The entanglement of the filaments therefore prevents the reformation of the original closed paired SH residues between the crystalline filaments and only a few closed SH residues remain that can, upon reoxidation, form S–S bonds between the crystalline filaments. In initiation of disorganization, it is speculated that cleavage of the crosslinks that join phase C with phase M are reduced at this point, because they seemed to be the most resistant to reduction and correspond to approximately 11.9% of the internal filaments in phase M, as estimated by Naito and Arai.

The overall result would be a steep decline in the value of the Young's modulus at Pa = 80%.

If this proposed mechanism is correct, then avoidance of the disorganization caused by the fission of the crosslinks between phases C and M would be critical. A study of the

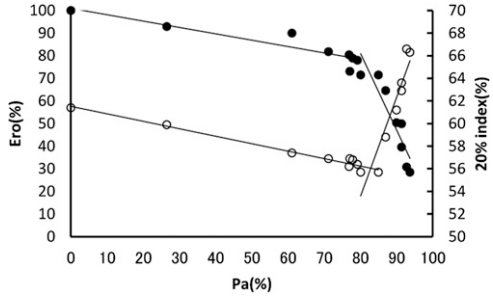

Figure 13. Relationship between Pa and both the Ero and the 20% index during extensional permanent treatment using the same hairs (●) Ero (left axis) and (○) 20% index (right axis). Note: Both the Ero and 20% index values simultaneously changed at approximately 80% of Pa.

characteristics of these crosslinks may therefore lead to the development of new wave lotions that result in a reduced level of hair damage.

ACKNOWLEDGMENTS

The authors thank Drs. K. Murakami, H. Oikawa, K. Arai, and K. Kawamura for assistance with this manuscript. We also acknowledge the kind support of our colleagues at formerly named Mitsui Petrochemical Industries Ltd, prior to the merger with Mitsui Chemical Ltd. Moreover, we thank the young female students at Toyama Senior High School for agreeing to donate virgin hair samples, and Dr. S. Roeper for providing the German lady's virgin hair. We also gratefully acknowledge the cooperation of the beauty parlors, BOY and ADOMI. Finally, the authors thank Enago (www.enago.jp) for the English review.

REFERENCES

(1) K. Arai, "Physical and chemical properties of wool and human hair" in *Newest Hair Science*, 1st Ed T. Matsuzaki, K. Arai, K. Jookoo, M. Hosokawa, and K. Nakamura. Eds. (Fragrance Journal LTD., Tokyo, 2003), 1st Ed., pp. 59–153.
(2) C. R. Robbins, *Chemical and Physical Behaviour of Human Hair*, 4th Ed. (Springer, New York, 2002), pp.225–288.
(3) D. E. Deem and M. M. Rieger, Mechanical hysteresis of chemically modified hair, *J. Cosmet Sci.*, **19,** 395–410 (1968).
(4) F.-J. Wortmann and I. Souren, Extensional properties of human hair and permanent waving, *J. Cosmet Sci.,* **38,** 125–140 (March/April 1987).
(5) A. V. Tobolsky, *Mechanische Eigenschaften und Struktur von Polymeren* (Berliner Union, Stuttgart, 1967).
(6) G. A. Etlmann, Die modenen Dauerwellsysteme, *Parfumerie und Kometik*, **64,** 541–544 (1983).
(7) J. Y. Dai, K. Li, P. F. Lee, X. Zhao, and S. Redkar, STEM study of interfacial reaction at $Hf_xAl_{1-x}Oy/Si$, *Thin Solid Films*, **462–463,** 114–117 (2004).
(8) E. F. Denby, A note on the interconversion of creep, relaxation and recovery, *Reol Acta*, **14,** 591–593 (1975).

(9) S. De Jong, Linear viscoelasticity applied to wool setting treatments, *Text Res J.* **55,** 647–653 (1985).
(10) F.-J. Wortmann and N. Kure, Bending relaxation properties of human hair permanent waving performance, *J. Cosmet Sci,* **41,** 123–139 (March/April 1990).
(11) R. R. Wickett, Kinetic studies of hair reduction using a single fiber technique, *J. Cosmet Sci.*, **34,** 301–316 (September/October 1983).
(12) M. A. Manuszak, E. T. Borish, and R. R. Wickett, Kinetics of disulfide bond reduction in hair by ammonium thioglycolate and dithioglycolate, *J. Cosmet Sci.*, **47,** 49–58 (1998).
(13) J. P. Danehy and C. J. Noel, The relative nucleophilic character of several mercaptans toward ethylene oxide, *J. Am Chem Soc.*, **82,** 2511–2515 (1960).
(14) R. H. De Deken, Étude Spectrophotomérique de la dissociation de la fonction sulfhydrule et structure moléculaire de la cystéine, Biochimica et Biophysica Acta, **19,** 45–51 (1956).
(15) M. L. Garcia, E. M. Nadgorny, and L. J. Wolfram, Physicochemical changes in hair during permanent waving, *J. Cosmet Sci.,* **41,** 149–154 (1990).
(16) A. Kazuhara and T. Hori, Reduction mechanism of L-cysteine on keratin fibers using microspectrophotometry and Raman spectroscopy, *Biopolymer,* **79,** 324–554 (2005).
(17) M. Feughelman, A comment in "Bending relaxation in properties of human hair and permanent waving performance," *J. Cosmet Sci.*, **42,** 129–131 (1991).
(18) W. Stricks, I. M. Kolthoff, and N. Tanaka, The polarographic and amperometric determination of disulfide groups, *Anal Chem.*, **26,** 299–303 (1954).
(19) M. Feughelman, A two-phase structure for keratin fibers, *Text Res J.*, **29,** 223–228 (1959).
(20) S. Naito, K. Arai, M. Hirano, N. Nagasawa, and M. Sakamoto, Number, type and location of crosslinks in hair structure of keratin. V. number and type of crosslinks in microstructure of untreated potassium cyanide treated human hair, *J. Appl Polym Sci.*, **61,** 1913–1925 (1996).
(21) Y.Ueno, U.S.Patent, No. 5,080,890, January 14, 1992.